J|A|C|S COMMUNICATIONS

Published on Web 07/28/2006

Transferring Self-Assembled, Nanoscale Cables into Electrical Devices

Shengxiong Xiao,[†] Jinyao Tang,[†] Tobias Beetz,[‡] Xuefeng Guo,[†] Noah Tremblay,[†] Theo Siegrist,[§] Yimei Zhu,[‡] Michael Steigerwald,[†] and Colin Nuckolls*,[†]

Department of Chemistry and Center for Electronics of Molecular Nanostructures, Columbia University, New York, New York 10027, Center for Functional Nanomaterials, Brookhaven National Laboratory, Upton, New York 11973-5000, and Bell Laboratories, Lucent Technologies, 600 Mountain Avenue, Murray Hill, New Jersey 07974

Received June 15, 2006; E-mail: cn37@columbia.edu

Here we describe the synthesis, self-assembly, and properties of the contorted hexabenzocoronenes[1] (HBC) **1**. We show that this material organizes into molecular stacks, and further that these stacks organize into cables or fibers.[2−5] These cables are ordered both on the molecular scale and on the supramolecular scale having an orthorhombic unit cell of 5.8 nm × 4.5 nm × 0.45 nm. We exploit this self-assembly process and the integrity of the resulting long-range order through the use of an elastomeric stamp to pick individual cables out of tangled mats and place them into electrical test structures.[6] This pick-and-place procedure yields field effect transistors[7−9] constructed from isolated nanoscale fibers. This study utilizes the power of self-assembly to create highly ordered nanostructured materials and develops a general method to manipulate and position them in devices.

Prior to this study, octa-substituted derivatives of the HBCs, such as **1**, had not been prepared, but their synthesis follows the procedure developed for the tetrasubstituted versions.[1] The strain in the periphery of these compounds creates structures that are bent[2,10,11] significantly away from planarity. Experimental details and spectroscopic characterization used for the synthesis of **1** are contained in the Supporting Information.

Unlike the material with four alkoxyl side chains, which shows a columnar liquid crystalline phase,[1] differential scanning calorimetry (in the Supporting Information) for **1** shows no evidence of a mesophase. This compound does organize supramolecularly; it forms crystalline fibers when its solutions in dodecane are concentrated by evaporation. Adjusting the solvent, temperature, and concentration, we have coarse control over the dimensions of the fibers. A movie showing the self-assembly of **1** into fibers is contained in the Supporting Information. The fibers shown in Figure 1B were grown from dodecane (2 mg/mL) over the period of a few days. Each of the fibers is ∼200 nm wide, implying that a few thousand molecular strands of 5 nm in diameter would pack to form the nanostructures.

We used transmission electron microscopy (TEM), electron diffraction, and powder X-ray diffraction to elucidate the structure of the fibers. Figure 2A and B shows TEM micrographs of fibers grown on a lacey carbon grid. To circumvent the extreme sensitivity of these fibers to the incident electrons, a CCD camera was used to continuously record the diffraction patterns while the sample was moved through the electron beam. Figure 2C shows an electron diffraction pattern from a *single* HBC fiber similar to the one in Figure 2B. The exposure time to record the pattern was 0.1 s. The electron diffraction pattern features diffraction spots along three lines, indicated by (*hk*0), (*hk*1) and (*hk*−1), which extend perpendicular to the direction of the fiber. The distance between the lines gives the unit cell spacing along the *c*-axis (0.45 nm). If this distance

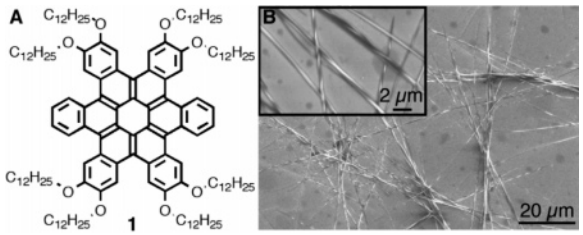

Figure 1. (A) Octa-substituted HBC **1**. (B) SEM of a mat of fibers grown from dodecane solution of **1** (inset: higher magnification micrograph).

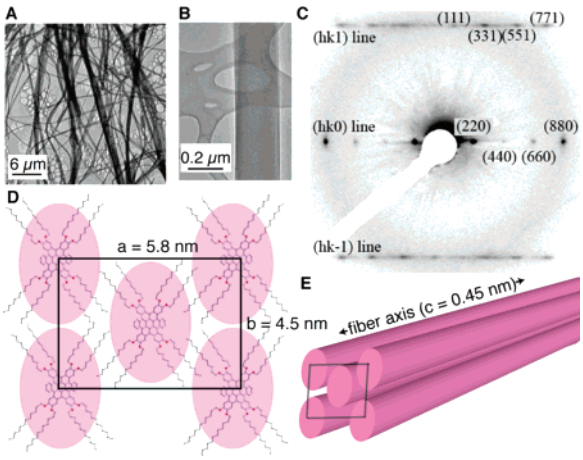

Figure 2. (A) TEM images of fibers of **1** on a lacey carbon grid. (B) Higher magnification image of an individual fiber. (C) Electron diffraction pattern from a single HBC fiber. (D) Rectangular arrangement of **1**. (E) Packing of the columns into a fiber along the *c*-axis.

is the π-to-π, intermolecular spacing, it is atypically large (typically ∼3.5 Å). The intermolecular nestling that is required for the contorted core of **1** to stack forces the arenes to offset from one another in adjacent molecules, but the π-to-π distance is significantly less than 0.45 nm.

An overall pseudohexagonal arrangement of the HBC core is then assumed,[1] further modified by the alkane chains, consistent with the electron diffraction pattern, and an orthorhombic unit cell with approximate dimensions of 6.0 nm × 4.5 nm × 0.45 nm was inferred. A full pattern fit using the program Winprep[12] of the powder X-ray diffraction data gave a refined orthorhombic unit cell with dimensions of $a = 5.8$ nm, $b = 4.5$ nm, and $c = 0.45$ nm. The most intense peak corresponds to a spacing ($d = 4.3$ nm) roughly the same as the long axis of the oval-shaped, HBC disk with its side chains fully extended. If we assume this reflection to be from the *b*-axis of the orthorhombic lattice and further assign the second most intense reflection ($d = 1.8$ nm) the index (220), the remaining reflections in the diffraction pattern refine well.

Fibers have been formed from flat HBCs[13,14] prepared by Aida and co-workers.[3] These materials organize into two-dimensional

[†] Columbia University.
[‡] Brookhaven National Laboratory.
[§] Lucent Technologies.

10.1021/ja0642360 CCC: $33.50

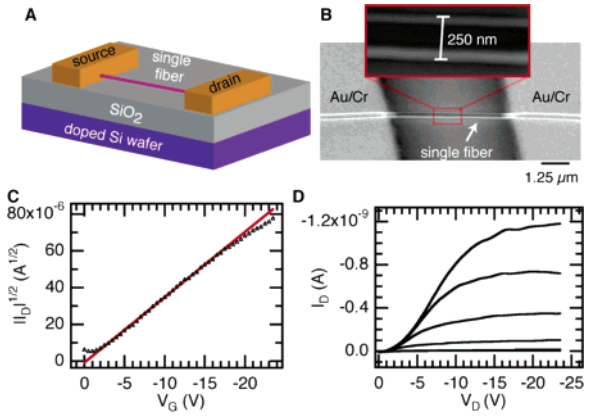

Figure 3. (A) Schematic of a FET from an isolated fiber. (B) Micrograph of a device formed from an isolated fiber that spans Au (200 nm thick) on Cr (5 nm thick) electrodes. The silicon wafer forms a back gate for the device. (C) Transfer characteristics ($V_{DS} = -50$ V) and (D) transistor output. $V_G = 0$ and -24 V in 4 V steps. The electrical characteristics are for the device pictured in (B).

sheets because the molecules are substituted to be amphiphilic. These sheets then roll themselves into a hollow helix. In our present case, the structure is much different: the columns are solid rods rather than hollow tubes. The oval cross section of the columns causes them to pack into a rectangular lattice, as shown in Figure 2D,E. By aligning the fibers in devices, we can probe the electrical conductivity along the one-dimensional stacks where they should be most highly conductive.[15,16]

We developed a method to manipulate, align, and transfer isolated fibers into transistor devices using elastomer stamps. This technique follows those developed for carbon nanotubes[6,17] and nanowires.[18,19] First, we grow a mat of nanofibers from dodecane solution (shown in Figure 1B) by slow evaporation of the solvent. An elastomer stamp made from polydimethoxysilane (PDMS) is gently pressed into the mat of fibers. Remarkably only a few fibers transfer to the stamp. Pressing the "loaded" stamp onto a substrate or device test structure then transfers this fiber.

We tested two methods for making devices out of these fibers. One was to transfer the fibers onto prefabricated electrodes, and another was to transfer the fiber to a clean wafer and then evaporate electrodes onto them through a shadow mask (100 μm $\times$ 100 μm squares separated by 5 μm). We found better electrical characteristics when the fibers were first transferred and the electrodes subsequently deposited.

A device constructed on an individual fiber and its electrical characteristics are shown in Figure 3. The material behaves as a p-type, hole-transporting semiconductor. The length of the fiber spanning the Au/Cr electrodes is 6.1 μm, and its width is $\sim$250 nm. The carrier mobility in these fibers is estimated to be $\sim$0.02 cm^2/V·s.[20] These values are quite good compared to other columnar materials[1,21,22] but are still a lower limit on the values that are possible with these materials. The nonlinear current voltage curves at low V_D in Figure 3D indicate they are limited by contact resistance.[23,24] Moreover, the drain current in the gate sweep (Figure 3C) is greater than that in the corresponding source-drain sweep (Figure 3D), indicating there is a measurable amount of carrier trapping.[25,26] We tested around a 100 devices made from fibers and found that the mobility varied sample to sample, ranging between 10^{-4} and $\geq 10^{-2}$ cm^2/V·s. This variation is likely due to the differences in morphology of individual fibers (as seen in Figure 1B) and changes in the physical contact to each of the fibers.

This study describes two new items: one is material, a new set of molecules that self-organize into molecular cables, and the other is methodological, where we use elastomer stamps to pick-and-place self-organized organic cables into devices. It would have been difficult to study the former without the latter, as it would be difficult to exploit the latter without a material like **1**. This method is broadly applicable in materials chemistry for testing the properties of individual, self-assembled organic nanostructures and the elucidation of intrinsic properties.

Acknowledgment. We acknowledge support from the Nanoscale Science and Engineering Initiative of the NSF under Award Number CHE-0117752 and by the New York State Office of Science, Technology, and Academic Research (NYSTAR); the DOE, Nanoscience Initiative (NSET#04ER46118); the NSF CAREER award (#DMR-02-37860). We thank the MRSEC Program of the NSF under Award Number DMR-0213574 and by the New York State Office of Science, Technology and Academic Research (NYSTAR). The work at Brookhaven National Laboratory was supported by the Office of Basic Energy Sciences, U.S. DOE. This manuscript has been authored by Brookhaven Science Associates, LLC under Contract No. DE-AC02-98CH10886 with the U.S. DOE.

Supporting Information Available: Experimental details for synthesis, structure determination, and electrical measurements, and a movie showing the self-assembled fiber growth. This material is available free of charge via the Internet at http://pubs.acs.org.

References

(1) Xiao, S.; Myers, M.; Miao, Q.; Sanaur, S.; Pang, K.; Steigerwald, M. L.; Nuckolls, C. *Angew. Chem., Int. Ed.* **2005**, *44*, 7390−7394.
(2) Lovinger, A. J.; Nuckolls, C.; Katz, T. J. *J. Am. Chem. Soc.* **1998**, *120*, 264−268.
(3) Hill, J. P.; Jin, W.; Kosaka, A.; Fukushima, T.; Ichihara, H.; Shimomura, T.; Ito, K.; Hashizume, T.; Ishii, N.; Aida, T. *Science* **2004**, *304*, 1481−1483.
(4) Kato, T.; Mizoshita, N.; Moriyama, M.; Kitamura, T. *Top. Curr. Chem.* **2005**, *256*, 219−236.
(5) Bushey, M. L.; Nguyen, T.-Q.; Zhang, W.; Horoszewski, D.; Nuckolls, C. *Angew. Chem., Int. Ed.* **2004**, *43*, 5446−5453.
(6) Huang, X. M. H.; Caldwell, R.; Huang, L.; Jun, S. C.; Huang, M.; Sfeir, M. Y.; O'Brien, S. P.; Hone, J. *Nano Lett.* **2005**, *5*, 1515−1518.
(7) Dimitrakopoulos, C. D.; Malenfant, P. R. L. *Adv. Mater.* **2002**, *14*, 99−117.
(8) Horowitz, G. *Adv. Mater.* **1998**, *10*, 365−377.
(9) Garnier, F. *Chem. Phys.* **1998**, *227*, 253−262.
(10) Wang, Z.; Doetz, F.; Enkelmann, V.; Muellen, K. *Angew. Chem., Int. Ed.* **2005**, *44*, 1247−1250.
(11) Wurthner, F. *Chem. Commun.* **2004**, 1564−1579.
(12) A full pattern fit was used to refine the unit cell parameters, giving an overall agreement factor Rwp = 0.17% (program "Winprep" 2005-02-14; diffraction pattern modifier by Kenny Stahl, Department of Chemistry, Technical University of Denmark, DK-2800 Lynby, Denmark; kenny@kemi.dtu.dk). See the Supporting Information.
(13) Cavallini, M.; Stoliar, P.; Moulin, J.-F.; Surin, M.; Leclere, P.; Lazzaroni, R.; Breiby, D. W.; Andreasen, J. W.; Nielsen, M. M.; Sonar, P.; Grimsdale, A. C.; Mullen, K.; Biscarini, F. *Nano Lett.* **2005**, *5*, 2422−2425.
(14) Kastler, M.; Pisula, W.; Wasserfallen, D.; Pakula, T.; Muellen, K. *J. Am. Chem. Soc.* **2005**, *127*, 4286−4296.
(15) Boden, N.; Bushby, R. J.; Lozman, O. R. *Mol. Cryst. Liq. Cryst.* **2003**, *400*, 105−113.
(16) Piris, J.; Debije, M. G.; Stutzmann, N.; van de Craats, A. M.; Watson, M. D.; Muellen, K.; Warman, J. M. *Adv. Mater.* **2003**, *15*, 1736−1740.
(17) Meitl, M. A.; Zhou, Y.; Gaur, A.; Jeon, S.; Usrey, M. L.; Strano, M. S.; Rogers, J. A. *Nano Lett.* **2004**, *4*, 1643−1647.
(18) Sun, Y.; Rogers, J. A. *Nano Lett.* **2004**, *4*, 1953−1959.
(19) Menard, E.; Lee, K. J.; Khang, D.-Y.; Nuzzo, R. G.; Rogers, J. A. *Appl. Phys. Lett.* **2004**, *84*, 5398−5400.
(20) The mobility is calculated by plotting $|I_D|^{1/2}$ with $|V_G|$ and using the equation: $I_D = (W \cdot C_i/2 \cdot L)(V_G - V_0)^2$; W is the width and L is the length; the source-drain voltage is fixed at -50 V (in the saturation regime of the $I-V$ curves in Figure 3D). For the 100 nm SiO_2 layer, $C_i = 33$ nF/cm^2.
(21) van de Craats, A. M.; Warman, J. M.; Fechtenkotter, A.; Brand, J. D.; Harbison, M. A.; Mullen, K. *Adv. Mater.* **1999**, *11*, 1469−1472.
(22) Pisula, W.; Menon, A.; Stepputat, M.; Lieberwirth, I.; Kolb, U.; Tracz, A.; Sirringhaus, H.; Pakula, T.; Muellen, K. *Adv. Mater.* **2005**, *17*, 684−689.
(23) Pesavento, P. V.; Chesterfield, R. J.; Newman, C. R.; Frisbie, C. D. *J. Appl. Phys.* **2004**, *96*, 7312−7324.
(24) Blanchet, G. B.; Fincher, C. R.; Lefenfeld, M.; Rogers, J. A. *Appl. Phys. Lett.* **2004**, *84*, 296−298.
(25) Lang, D. V.; Chi, X.; Siegrist, T.; Sergent, A. M.; Ramirez, A. P. *Phys. Rev. Lett.* **2004**, *93*, 076601.
(26) Chang, J. B.; Subramanian, V. *Appl. Phys. Lett.* **2006**, *88*, 233513.

JA0642360